Design of All-Dielectric 2D Periodic Structure Supporting Bound State in Continuum at a Prescribed Frequency

Design of All-Dielectric 2D Periodic Structure Supporting Bound State in Continuum at a Prescribed Frequency

Aldo De Sabata[(1)], Ovidiu Z. Lipan [(2)], and Ladislau Matekovits[(3)]

(1) Politehnica University Timisoara, Romania, Timisoara, Romania (aldo.de-sabata@upt.ro)
(2) University of Richmond, Richmond, VA, USA (olipan@richmond.edu)
(3) Politecnico di Torino, Torino, Italy (ladislau.matekovits@polito.it)

***Abstract*— Bound states in the continuum (BIC) have recently gained significant attention within the research community. In this work, we propose a design procedure to achieve a structure that supports a BIC at a specified frequency, eliminating the need for optimization-based or heuristic approaches. The procedure leverages closed-form formulas for the transfer matrix, which relates the Bloch-Floquet modes on both sides of an all-dielectric, two-dimensional periodic structure. The proposed methodology is demonstrated through an example that generates a BIC at 10 GHz, with its performance validated by full-wave simulations, and whose geometry can be conveniently scaled to operate at other desired frequencies.**

I. Introduction

Purposely designed all-dielectric, two-dimensional periodic structures support bound states in the continuum (BICs), which are electromagnetic modes that belong to the radiation continuum. These modes propagate within the structure but do not radiate energy. A significant class of BICs is protected by symmetry; however, when the symmetry is broken, these propagation modes couple with incident plane waves, transforming into quasi-BICs [1].

Structures supporting BICs are typically designed to operate in the THz frequency range, finding applications in sensors, lasers, and related technologies [2-6]. Designing structures that support a BIC at a specific frequency is a challenging task, often addressed through geometry and material optimization or other ad-hoc methods.

In contrast, this paper proposes a systematic design procedure based on closed-form formulas derived from electromagnetic theory. These formulas enable direct determination of the geometrical and material parameters required for a structure to support a BIC at a desired frequency.

Our approach uses closed-form expressions for the transfer matrix, which relates the fields incident on the periodic structure to the diffracted fields, expressed in the Bloch-Floquet basis [7]. The key equations governing the geometrical and material parameters needed to achieve a BIC in the specific structure considered here are detailed in [8].

In this paper, we introduce a systematic design methodology and provide an illustrative example involving a structure that supports a BIC at a prescribed frequency in the GHz range—a location less commonly explored in the existing literature.

The remainder of the paper is organized as follows: Section II introduces the unit cell of the 2D periodic structure and defines its geometrical and material parameters. Section III outlines the design procedure, details the parameters constraints, and presents an example solution that supports a BIC at 10 GHz. Section IV validates the proposed solution through simulations. The conclusions are presented in the last section.

II. Unit Cell Structure and Design Parameters

The design of the unit cell is represented in Fig. 1. It consists of a square dielectric slab with a relative permittivity of ε_B, featuring a square hole where the permittivity equals that of free space. The edge of the unit cell, denoted L_y represents one of the design parameters (Fig. 1 (a)). The other parameter is the thickness of the structure, Fig. 1 (b), introduced as a fraction ζ of L_y. The objective is to determine L_y, ζ, and ξ (the ratio of the square hole's edge length to the unit cell's edge length), ensuring the structure supports a BIC at a specified frequency. However, care must be taken to ensure proper discretization of the z-axis, as one of the key steps in deriving the closed form of the transfer matrix in [7] involved discretizing the propagation (z) axis, leading to the first order approximation:

$$igk_z \approx e^{igk_z} - 1, \tag{1}$$

where $k_z = \frac{2\pi}{\lambda}\cos(\theta)$ is the longitudinal wavenumber, λ is the free-space wavelength, θ is the angle of incidence and g is the half thickness of the structure (equal to $\frac{1}{2}\zeta L_y$ in this case). Denote:

$$\Omega = \frac{2\pi g}{\lambda} = \pi\zeta\frac{L_y}{\lambda} \tag{2}$$

The relative error that occurs by replacing the LHS by the RHS in (1) is represented in Fig. 2 for the case of a normal incidence (a one-to-one correspondence is achievable for

$|\Omega| < \pi$, however an upper limit of 0.02 has been chosen for the representation). The parameter Ω defined in (2) is relevant for the theory proposed in [7], where it plays the role of a normalized, unitless frequency.

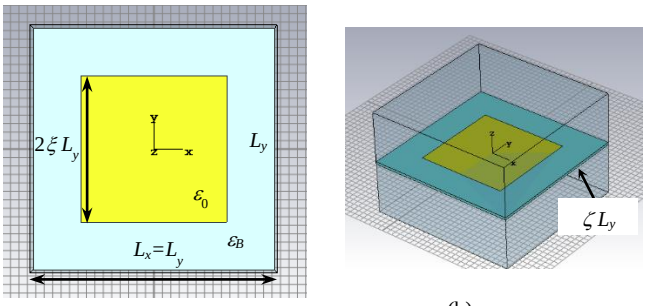

(a) (b)

Fig. 1. CAD image of the unit cell: (a) front view; (b) perspective.

Minimizing errors resulting from sampling along the *z*-axis requires a small value of Ω, which may impose constraints on the design procedure. However, this condition is readily fulfilled by choosing a unit cell with dimensions of the order of the wavelength, since $\zeta << 1$ due to the way the *z*-axis is discretized in [7]. Therefore, the design parameters to be found are ξ, L_y and ζ. The normalized frequency Ω results from (2).

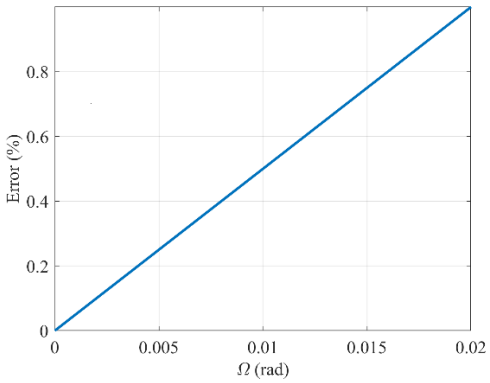

Fig. 2. Percentage error introduced by the discretization of the *z* axis.

III. Design Procedure

The equations that are associated with BIC-carrying device having the structure of the unit cell in Fig. 1 are as follows [8].

Denote

$$W = \zeta\pi\,, \tag{3}$$

$$z = \frac{1}{2}\left(2 + W^2 - \Omega^2\right), \tag{4}$$

$$\varphi_e = z - \sqrt{z^2 - 1}\,. \tag{5}$$

Let

$$F(\xi) = \xi^2\left(1 - \mathrm{sinc}(4\xi)\right),\ \mathrm{sinc}(\xi) = \frac{\sin(\pi\xi)}{\pi\xi} \tag{6}$$

$$0 < \xi < 1$$

Note that $F(\xi)$ increases from 0 to 1 as ξ goes from 0 to 1.

Let

$$G = \frac{1}{4}\frac{\left[(\varepsilon_B - 1)\Omega^2\varphi_e - 1\right]^2 - \varphi_e^2}{\left[(\varepsilon_B - 1)\Omega^2\varphi_e - 1\right]^2 - 1}. \tag{7}$$

If the following equation is verified, then the structure supports a BIC [8]:

$$F(\xi) = G\,. \tag{8}$$

For a given dielectric constant ε_B, this equation can be solved numerically for ξ in terms of L_y and ζ. Solutions exist only when $0<G<1$.

Furthermore, to have a solution, φ_e must be real. From (4) and (5), we get $z > 1$ and $W > \Omega$, so that

$$L_y < \lambda\,. \tag{9}$$

Although (9) allows for λ to be significantly larger that L_y, it later becomes evident that these two values are close to each other.

Also $\Omega < \pi\zeta$, which is convenient, since we assumed ζ to be small, so that Ω is also small.

Suppose the goal is to achieve a BIC at a target frequency *f* (10 GHz in this example), using the device shown in Fig. 1, having $\varepsilon_B = 11.9$, $L_y = 28.6$ mm, and $\zeta = \frac{1}{60}$. Fig. 3 illustrates the right-hand side (RHS) and left-hand side (LHS) of (8) as functions of ξ, demonstrating the existence of a solution, namely $\xi = 0.2983$.

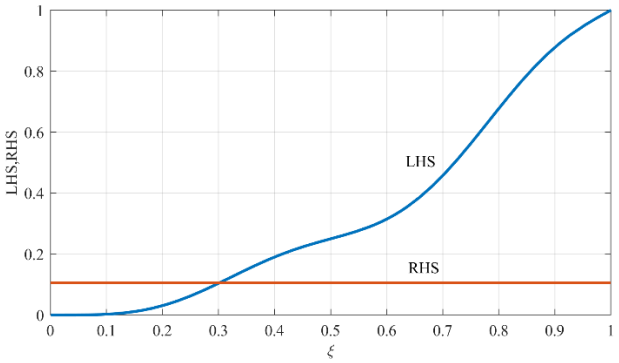

Fig. 3. Right-hand side (RHS) and left-hand side (LHS) of (8) as functions of ξ.

Equation (8) does not admit a solution ξ between 0 and 1 for all the possible dimensions of the unit cell. This is illustrated in Fig. 4, which represents the solution as a function of L_y/λ (which must be smaller than 1, see (9)), and ζ between 0.01 and 0.1. The absence of a solution is indicated by $\xi = 0$ in Fig. 4.

To provide a more useful design guideline, the curve in the $(L_y/\lambda, \zeta)$ plane that separates regions where solutions for (8) exist (marked by "BIC") from regions of no-solution (marked by "No BIC") are represented in Fig. 5, for several values of the dielectric constant ε_B. It is important to note that the absence of BICs pertains specifically to the procedure considered here. BICs arising from other sources may still exist. Moreover, higher values of the dielectric constant (above about 22.5) slightly modify the shape of the regions. We restrict this analysis to ε_B<21 for brevity. Extending it to larger dielectric constant is straightforward.

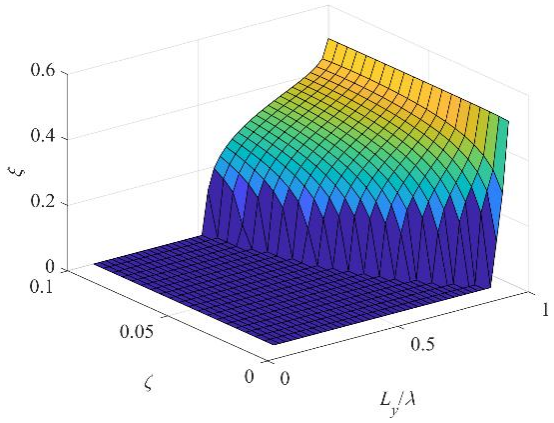

Fig. 4. Solution of (8) for various unit cell dimensions.

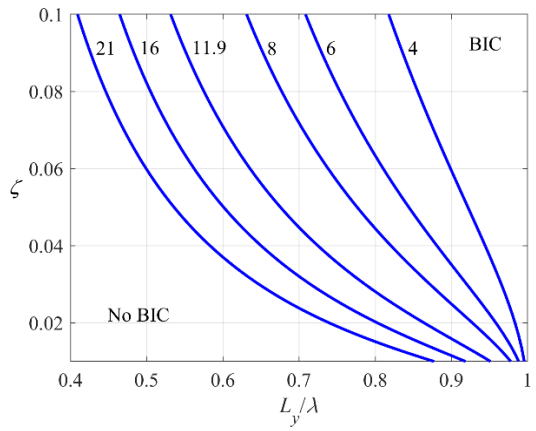

Fig. 5. Curves separating regions in the parameter plane that determine whether solutions to (8) exist, parametrized by ε_B.

To summarize the design procedure: Given the desired frequency for the BIC, select ε_B, L_y, and ζ to meet the particular technical constraints of the application and ensure that the pair $(L_y/\lambda, \zeta)$ lies within the appropriate region in Fig. 5. Then, solve (8) to determine ξ.

IV. Validation by Simulation

The design example from Section III has been tested through full-wave simulations performed using [10]. The obtained transmission coefficient is reported in Fig. 6, for a frequency range 1 GHz-wide around the central frequency of 10 GHz, which was selected to carry the BIC, and for three values of the angle of incidence θ close or equal to zero. A total of 40 modes were included in the simulations.

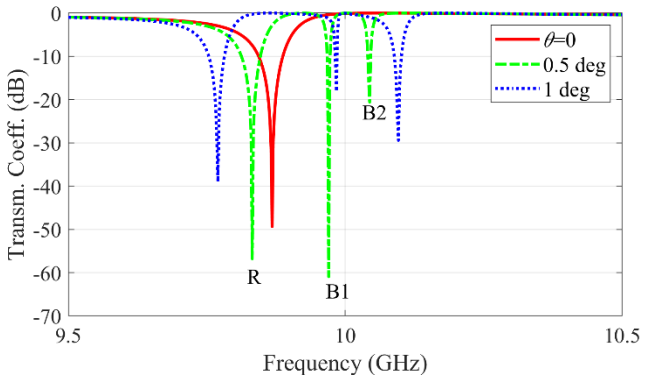

Fig. 6. Transmission coefficient vs. frequency parametrized by the incidence angle. The resonance is denoted as R, while B1 and B2 represent quasi-BICs. Quasi-BICs emerge when the incidence angle θ exceeds zero ($\theta > 0$).

The transmission coefficient features three notches when symmetry is broken (θ>0), denoted by R, B1, and B2 on the curve corresponding to θ=0.5°. These results are in accordance with [8], where working frequencies were in the THz range. The notch denoted by R, occurring at 9.83 GHz, is a resonance, since it does not vanish when symmetry is restored (θ=0). This resonance is stable and it features a discernable shift in frequency up to angles of incidence of 85° [9]. B1 and B2 are quasi-BICs, since they vanish at θ=0, indicating the transition of the device from opacity to transparency when the symmetry is restored. B1 occurs at 9.97 GHz and B2 occurs at 10.04 GHz for θ=0.5°. The values for θ=1° are 9.98 and 10.10 GHz respectively. The resonance R occurs at 9.86 and 9.77 GHz for θ=0 and 1° respectively.

The design procedure for obtaining a BIC-carrying structure, as developed in [8] using the transfer matrix method, relied on five modes deemed relevant. It was also demonstrated that the designed BIC splits into two BICs when a sufficiently large number of modes is included in simulations, with results stabilizing as the number of modes is increased. This behavior has been confirmed in this study. The error in positioning the BIC at 10 GHz is approximately 0.3%.

It is worth mentioning that the design procedure introduced here establishes a direct proportionality between the unit cell's edge L_y and the BIC frequency provided the parameters ξ and ζ remain fixed. For instance, halving the value of L_y from the example in Section III results in a BIC frequency of 5 GHz, while increasing L_y by a factor of 3/2 raises the BIC frequency to 15 GHz. These findings have been validated through full-

wave simulations, as illustrated in Table I, where the notations for the resonance and the two quasi-BICs correspond to those in Fig. 6.

TABLE I. FREQUENCIES AND TRANSMISSION COEFFICIENTS OF THE RESONANCE (R) AND QUASI-BICS (B1 AND B2) FOR AN OBLIQUE INCIDENCE AT θ=0.5°

L_y (mm)	R	B1	B2
14.3	4.92 GHz -57.03 dB	4.98 GHz -11.77 dB	5.02 GHz -19.14 dB
42.9	14.75 GHz -51.61 dB	14.96 GHz -21.05 dB	15.07 GHz -25.87 GHz

V. CONCLUSIONS

We have introduced a systematic procedure for designing a 2D periodic structure that supports a BIC at a specified frequency. The structure comprises a dielectric layer with perforated holes, a configuration commonly employed in BIC applications. Our method is founded on a closed-form formula for the transfer matrix, eliminating the need for optimization or trial-and-error techniques.

The proposed approach includes an equation that determines the dimensions of the holes based on permissible values of the geometric parameters, which are specified within provided ranges. Notably, the edge length of the square unit cell must be smaller than but close to the wavelength corresponding to the design frequency.

We have provided an example of a structure supporting a BIC at 10 GHz and showed that its geometry can be conveniently scaled to operate at other desired frequencies.

REFERENCES

[1] C.W. Hsu, B. Zhen, A. D. Stone, J.D. Joannopoulos and M. Soljacic, "Bound states in the continuum," *Nat. Rev., Mater.*, 16048, July, 2016.

[2] W. Wang, Y.K. Srivastava, T.C. Tan, Zh. Wang, and R. Singh, "Brillouin zone folding driven bound states in the continuum," *Nat. Comm.*, vol. 14, art. no. 2811, 2023.

[3] L. Yang, S. Yu, H. Li, and T.G. Zhao, "Multiple Fano resonances excitation on all-dielectric nanohole arrays metasurfaces," *Opt. Exp.*, vol. 29, no. 10, pp. 14905-14916, May 2021.

[4] C. Zhao, Y. Huo, T. Liu, Z. Liao, C. Xu, and T. Zhang, "All-dielectric metasurface with multiple Fano resonances supporting high-performance refractive index sensing," *J. Opt. Soc. Am. B*, vol. 41, no. 1, pp. 36-45, Jan. 2024.

[5] J. Zhang, Y. Ruan, Z.-D. Hu, J. Wu, and J. Wang, "An Enhanced High Q-Factor Resonance of Quasi-Bound States in the Continuum With All-Dielectric Metasurface Based on Multilayer Film Structures," *IEEE Sensors J.*, vol. 23, no. 3, pp. 2070-2075, Feb. 2023.

[6] Y. Hu, S. Xie, C. Bai, W. Shen, and J. Yang, "Multiple Photonic Bound States in the Continuum in an Electromagnetically Induced Transparency Metasurface," *IEEE Phot. J.*, vol. 14, no. 4, art. no. 4641308, Aug. 2022.

[7] O.-Z. Lipan, and A. De Sabata, "Closed-form analytical solution for the transfer matrix based on Pendry-MacKinnon discrete Maxwell's equations", *Opt. Exp.*, no. 33, pp. 3777–3817, 2025.

[8] O-Z. Lipan, and A. De Sabata, "Bound states in continuum via singular transfer matrices", *Phys. Rev. A* (to be published).

[9] A. De Sabata, O.-Z. Lipan, and L. Matekovits, "Exploiting Analytic Transfer Matrices to Engineer Resonances in Patterned Dielectric Periodic Surfaces," *Proc. Int. Symp. Antennas Propag.*, Florence, Italy, Jul. 2024, pp. 1053-1054.

[10] Computer Simulation Technologies, CST 2024.